ORIGINAL PAPER

Aggregation of αSynuclein promotes progressive in vivo neurotoxicity in adult rat dopaminergic neurons

**Grit Taschenberger · Manuel Garrido ·
Yuliya Tereshchenko · Mathias Bähr ·
Markus Zweckstetter · Sebastian Kügler**

Abstract Fibrillar αSynuclein is the major constituent of
Lewy bodies and Lewy neurites, the protein deposits charac-
teristic for Parkinson's disease (PD). Multiplications of the
αSynuclein gene, as well as point mutations cause familial PD.
However, the exact role of αSynuclein in neurodegeneration
remains uncertain. Recent research in invertebrates has sug-
gested that oligomeric rather than fibrillizing αSynuclein
mediates neurotoxicity. To investigate the impact of αSyn-
uclein aggregation on the progression of neurodegeneration,
we expressed variants with different fibrillation propensities
in the rat substantia nigra (SN) by means of recombinant
adeno-associated viral (AAV) vectors. The formation of
proteinase K-resistant αSynuclein aggregates was correlated
to the loss of nigral dopaminergic (DA) neurons and striatal
fibers. Expression of two prefibrillar, structure-based design
mutants of αSynuclein (i.e., A56P and A30P/A56P/A76P)
resulted in less aggregate formation in nigral DA neurons as
compared to human wild-type (WT) or the inherited A30P
mutation. However, only the αSynuclein variants capable of
forming fibrils (WT/A30P), but not the oligomeric αSynuclein
species induced a sustained progressive loss of adult nigral
DA neurons. These results demonstrate that divergent modes
of αSynuclein neurotoxicity exist in invertebrate and mam-
malian DA neurons in vivo and suggest that fibrillation of
αSynuclein promotes the progressive degeneration of nigral
DA neurons as found in PD patients.

Keywords αSynuclein · Parkinson's disease ·
Aggregation · Adeno-associated virus · Substantia nigra

G. Taschenberger (✉) · M. Garrido · Y. Tereshchenko ·
M. Bähr · S. Kügler
Center of Molecular Physiology of the Brain at Department
of Neurology, University Medicine Göttingen,
Waldweg 33, 37073 Göttingen, Germany
e-mail: gtasche@gwdg.de

M. Zweckstetter
Department for NMR Based Structural Biology,
Max Planck Institute for Biophysical Chemistry,
37077 Göttingen, Germany

Present Address:
M. Garrido
Center for Neuroscience and Cell Biology of Coimbra,
Largo Marquês de Pombal, 3004-517 Coimbra, Portugal

Introduction

Parkinson's disease (PD) is the most prevalent neurodegen-
erative movement disorder, affecting more than 2% of
individuals over the age of 60 years. Pathological hallmarks
of the disease are the progressive loss of dopaminergic (DA)
neurons in the substantia nigra pars compacta (SNpc) and the
presence of proteinous aggregates termed Lewy bodies within
DA neurons, which are predominantly composed of fibrillar
αSynuclein [27]. Gene triplication and inherited mutations of
αSynuclein cause early-onset PD, demonstrating a crucial role
for αSynuclein in the etiology of the disease [11, 17]. How-
ever, how αSynuclein induces neurodegeneration remains as
elusive as its physiological function.

αSynuclein belongs to the class of intrinsically disordered
proteins in solution, but it adopts a partially folded structure
upon a variety of environmental stimuli [41]. While mem-
brane bound α-helical αSynuclein does not contribute to
aggregation and fibrillation [47], soluble folding intermedi-
ates are thought to be essential for the initiation of aggregation
of the protein by a cascade comprising initially soluble, then
insoluble oligomers, and finally fibrils as found in Lewy
bodies [13]. The predominant physiological species of
αSynuclein in cells and brain is a helically folded tetramer
with a low propensity to aggregate into fibrils [3].

Lewy bodies are usually found in living neurons and are also present in 10–15% of healthy, aged individuals [15, 18]. Considering Lewy bodies as a protective sink for misfolded proteins rather than a toxic entity is therefore an attractive, but controversially discussed hypothesis [20]. Given the strong indications that αSynuclein is causally involved in degeneration of nigral DA neurons, it seems likely that oligomeric αSynuclein rather than fibrillar aggregates are the mediators of neuronal death. Consequently, the "toxic oligomer" hypothesis was postulated [6, 42, 46]. This hypothesis gained further support by a recent study in several invertebrate and cell-culture model systems of PD which reported increased neurotoxicity upon over-expression of αSynuclein variants that exhibited increased propensity to form oligomeric, prefibrillar structures and decreased propensities to form fibrillar aggregates [22].

Considering that species like Drosophila and C. elegans do not express αSynuclein orthologs, assessing aggregate formation and correlating aggregates to neurodegeneration to evaluate their relevance for PD should ideally be performed in adult mammalian DA neurons. In addition, PD is a slowly progressing disorder and a correlation of αSynuclein aggregation with the progressive loss of nigral DA neurons has not been assessed so far. To evaluate long-term effects of αSynuclein aggregate formation on DA neuron survival, we expressed αSynuclein variants with different aggregation propensities in neurons of the rat SN and quantified the loss of DA neurons over a time course of 3.5 months. To interfere with aggregation, the single-proline mutation found in the familial A30P mutant was moved to a position within the β-sheet rich core of αSynuclein fibrils. The single-proline αSynuclein mutant A56P as well as the triple-proline mutant A30P/A56P/A76P (TP) showed drastically reduced propensity to form proteinase K (PK)-resistant aggregates in vitro and in vivo, confirming the prior characterization of the mutants as prefibrillar αSynuclein variants by biophysical methods and in invertebrates [22]. However, only the αSynuclein species with increased aggregation propensities, human wild-type (WT) and A30P, triggered a further progressing degeneration of nigral DA neurons, and WT αSynuclein showed the highest degree of neurotoxicity after longer term overexpression. Our findings suggest that fibril formation of αSynuclein promotes the progressive degeneration of nigral DA neurons as found in PD patients and show that invertebrate and mammalian DA neurons are differently vulnerable to αSynuclein aggregation.

Materials and methods

AAV-vector production

AAV2 serotype vectors were constructed to express the human WT αSynuclein, the inherited A30P mutation, the two pre-fibrillary αSynuclein mutants A56P and A30P/A56P/A76P (TP), and EGFP. AAV2 serotype vectors were prepared essentially as previously described [38]. Their genomes consisted of AAV2 ITRs, human synapsin-1 gene promoter driving expression of αSynuclein variants, WPRE for enhanced mRNA stability and bovine growth hormone polyadenylation site. For Western blot assessing expression levels, primary cortical neuronal cultures were prepared from rat embryos at E18. Western blotting and preparation of conditioned medium and cell extracts were performed according to the procedure described previously [26].

Stereotaxic injection and tissue processing

All surgical procedures, intracerebral stereotaxic vector injections into the left hemisphere SNpc (coordinates were AP: −5.3; ML: +2.2; DV: −7.7 mm, relative to bregma) and tissue preparations were performed as described [37]. Young adult female Wistar rats (250–280 g) were injected with a total of 2 μl containing 1.2×10^8 transducing units. Animals were sacrificed at 2, 4, 8 and 14 weeks after virus injection. 30-μm thick serial coronal sections from both the SN and striatum were collected on a cryostat (Leica) and processed for immunohistochemistry.

Immunohistochemistry

The following primary antibodies against αSynuclein were used: mouse anti-human LB509 and syn211 (1:500, Invitrogen), 5C2 (1:500, Santa Cruz), and mouse anti-αSynuclein (1:500, Clone 42, BD Transduction Laboratories) recognizing human and rat αSynuclein. Immunofluorescent visualization of DA neurons was performed with rabbit polyclonal antibody against tyrosine hydroxylase (TH, 1:1,000, AB152). Monoclonal anti-β-Tubulin was obtained from Sigma. Primary antibodies were applied for 48 h at 4°C followed by 1 h incubation at RT with secondary antibodies on free-floating sections. For indirect immunofluorescence and Western-blot analysis, secondary antibodies against rabbit or mouse IgGs and conjugated with Cy2, Cy3, or horseradish peroxidase were used (Dianova). For the SNpc, every fourth section was used for immunohisto-chemistry (−4.52 to −6.3 mm, relative to bregma). For the striatum, one rostral and one caudal section were processed for each condition. Bright-field and fluorescent images were taken on an Axioplan microscope equipped with a 16-bit greyscale CCD camera using AxioVision 4.6 software (Zeiss). Some sections were examined with a laser-scanning confocal microscope (Leica TCS SP5) or with an ApoTome (Zeiss).

Quantification of neurodegeneration

For the bright-field microscopy analysis, visualization of DA neurons was performed with rabbit polyclonal antibody against vesicular monoamine transporter 2 (VMAT2, AB1767, Chemicon). Sections were preincubated first with 3% H_2O_2/10% methanol for 5 min and then with 5% normal goat serum for 1 h before incubation with the primary antibody VMAT2 (1:3,000, 4°C, 48 h). Incubation with biotinylated secondary anti-rabbit antibody (1:250) at room temperature for 1 h was followed by the avidin–biotin complex (ABC, Vector laboratories) method. The reaction product was visualized using 3,3′-diaminobenzidine tetrachloride (DAB, Sigma) as a chromogen.

To estimate the total number of DA neurons, VMAT2-immunoreactive cells were counted by stereology in every fourth brain section in the region of the SNpc (10 sections throughout the SN). VMAT2-positive cells of the ventral tegmental area were excluded from counting. Cell counts were performed in a blind manner using the StereoInvestigator software (MicroBrightField, Bioscience). Unbiased stereological estimates of the total number of VMAT2-positive neurons per SNpc were obtained using the optical fractionator method [43]. Survival of DA neurons was analyzed at 2, 4, 8, and 14 weeks after vector administration, with exception of the EGFP group, which was sacrificed at the last time point only.

PK digest

Insolubility of the human αSynuclein aggregates was demonstrated utilizing a modified version of a PK digestion and immunohistochemistry protocol [12]. Free-floating sections collected from brains 2 and 4 weeks after viral-vector injection were digested in PBS containing 10 μg/ml PK (Invitrogen) for a period of 10 min at 55°C. Longer incubation times with PK resulted in disintegration of the tissue and were therefore avoided. Maximum incubation time and temperature were established in preliminary experiments. Control sections adjacent to the digested ones were incubated in PBS only. Sections were quenched with 3% H_2O_2/10% methanol for 8 min and processed for immunohistochemistry using the syn211 antibody, that recognizes human αSynuclein protein. Immunoreactivity was visualized with the Vector ABC DAB system. All slices were processed simultaneously under strictly the same conditions and image acquisition and measurements were performed with the exact same settings and parameters. Bright-field images of the SN were taken on an Axioplan microscope equipped with a $63\times$ oil immersion objective and using AxioVision software (Zeiss, Germany). Quantitative data were extracted with the MacBiophotonics ImageJ program (NIH,

Maryland, USA, http://rsb.info.nih.gov/ij/). To estimate the PK-resistant fraction of αSynuclein, we performed measurements in at least six randomly selected fields per image from at least six images each. Cell somata were excluded from the quantification of the neuropil. As transgene expression was restricted to the injected side in all animals, we used the uninfected contralateral hemisphere as well as EGFP transduced sections to set the lower threshold value to correct for non-specific background. The upper threshold value was defined in undigested control sections.

For Thioflavin-S (ThioS) staining, mounted sections were incubated with 0.05% ThioS (Sigma) in 50% ethanol for 8 min after a quenching procedure to reduce background autofluorescence [39] and antibody incubations. Sections were differentiated in two changes of 80% ethanol for 10 s each, washed three times in large volumes of PBS, incubated with DAPI for 5 min and washed again.

Statistical analysis

Multiple comparisons were made by one-way ANOVA followed by Tukey's honestly significant difference test. The unpaired t test with Welch correction was used for statistical comparison between two groups. Differences were considered significant at $p < 0.05$. Statistical tests were performed using the R software package [36].

Results

Diminished aggregate formation by prefibrillar αSynuclein variants in cultured neurons

The two rationally generated mutants A56P and TP [22], the inherited A30P mutation, human WT αSynuclein, and EGFP were expressed in cultured primary cortical neurons using AAV2 vectors. The functional titers of the recombinant viral vectors were equal, i.e., all vectors express the same amount of αSynuclein (Fig. 1a). To validate that the artificial, oligomeric mutants A56P and TP indeed showed strongly impaired aggregation, we assessed the generation of aggregated αSynuclein by probing its resistance against PK digestion. Protein lysates of transduced neurons were digested with PK for either 5 or 30 min and the percentage of PK-resistant αSynuclein was quantified as a measure of aggregate formation. All values were normalized to the respective control levels without digestion. While 18% of WT αSynuclein and 30% of A30P αSynuclein were resistant to PK-digestion, this fraction decreased to <5% for the A56P and TP mutants (Fig. 1b, c). This observation corroborates results obtained by earlier in vitro studies demonstrating that A56P and TP form less aggregates in solution than WT or A30P [22].
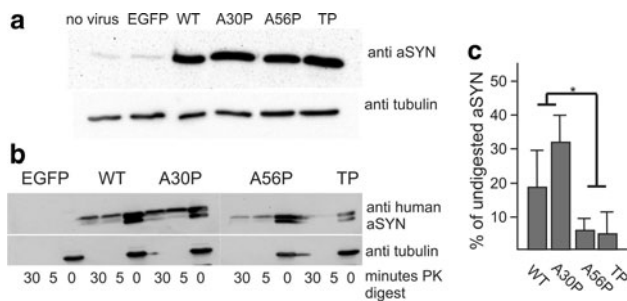
Fig. 1 Assessment of formation of PK-resistant aggregates in cultured primary neurons. **a** Western blot analysis of AAV2-expressed αSynuclein using total cell lysates from rat primary cortical neurons 6 days after transduction shows equal expression levels of all αSynuclein variants. Staining with antibody clone 42, which reacts with human and rat αSynuclein. **b** Western blot for αSynuclein on cell lysates from cortical neurons 6 days after transduction with AAV containing the different αSynuclein variants. The lysates were digested with PK for 0, 5, and 30 min. Staining with human specific antibody syn211. **c** Quantitative evaluation of band intensities of western blot analysis for 30 min PK digest. Formation of PK-resistant material given in % of undigested αSynuclein variant. Data given as mean ± SD from four independent experiments. *Asterisk* indicates a significant difference between groups ($p < 0.05$, paired *t* test)

Diminished aggregate formation by prefibrillar αSynuclein variants in adult DA neurons of the rat SNpc

We then assessed the formation of aggregates in midbrain tissue sections derived from adult rats by quantifying the amount of PK-resistant αSynuclein. These animals were injected into the SNpc with AAV vectors expressing WT, A30P, A56P or TP αSynuclein 4 weeks before tissue sampling. Control rats received identical injections of a AAV vector encoding EGFP. Tissue samples were subjected to the maximum possible dose and incubation time of PK, which was just below the threshold of completely digesting the tissue specimen. Untreated sections adjacent to the treated ones served as controls. This method has been shown to be the most sensitive procedure to detect αSynuclein aggregates in tissue specimen including post-mortem patient's brain [4, 32]. After immunohistochemistry with the human αSynuclein specific antibody syn211, PK-resistant aggregates were identified as small intensely stained inclusions of about 0.5 μm in diameter in cell bodies of DA neurons. The neuropil of untreated slices showed relatively large, focal bead-like swellings immunoreactive for αSynuclein. With PK treatment, we detected smaller profiles but with similar spatial arrangement (Fig. 2a–o). PK-resistant aggregates in the neuropil were quantified by calculating the fraction of αSynuclein-positive material using the ImageJ software. PK-resistant aggregates in neuronal cell bodies were quantified by counting of individual aggregates. Without PK treatment, αSynuclein immunoreactivity in the neuropil was

equal for all αSynuclein variants 4 weeks post transduction. Following PK treatment, WT and A30P expressing specimen demonstrated significantly higher levels of αSynuclein immunoreactivity as compared to A56P and TP (Fig. 2p). The number of PK-resistant intraneuronal αSynuclein aggregates was significantly higher in WT- and A30P-expressing neurons (99.1 ± 12 and 53.6 ± 20.6, respectively) compared to A56P- and TP-expressing neurons (5.9 ± 3.3 and 3.4 ± 3.8, respectively) (Fig. 2q). These PK-resistant aggregates did not co-stain with ThioS (Fig. 3). No aggregates were detectable in neurons of undigested sections, in PK-digested sections after EGFP overexpression or in the contralateral nigra (not shown). In contrast to the biochemical PK-resistance assay conducted with cell lysates from cultured non-DA cortical neurons, we found that expression of WT αSynuclein in adult rat DA neurons produced significantly more aggregates than expression of A30P, suggesting that the duration of the expression, the age of the neurons or the DA environment may differentially impact on aggregate formation.

To study the time course of aggregate formation in our in vivo model, we analyzed tissue sections obtained 2 weeks after viral-vector injection. Abnormally accumulated abundant cytoplasmic PK-resistant aggregates had already developed in nigral neurons overexpressing WT αSynuclein (Fig. 2r). The detected aggregates had, however, a smaller individual grain size compared with aggregates 4 weeks after injection.

As the aggregates were resistant to PK and thus likely consisted of fibrillar αSynuclein [8, 33], the extensive prior classification of WT and A30P αSynuclein as fibril-forming variants, and A56P and TP as fibrillization impaired variants [22] was confirmed in DA neurons of adult rats in vivo.

Only fibril-forming αSynuclein variants induce a long-lasting progression of DA neuron degeneration

Overexpression of WT, A30P, A56P, TP αSynuclein, and EGFP in rat nigral neurons was performed by means of an AAV2 serotype vector. The efficient transduction of all brains and expression of each construct was confirmed by immunohistochemistry. Neuronal localization of αSynuclein was studied by double immunofluorescence with the dopaminergic-specific marker TH (Fig. 4d–i). Due to the documented inhibitory effect of αSynuclein on TH expression [45], all cell counts were performed using immunohistochemistry for VMAT2 (Fig. 4l).

Survival of DA neurons was first analyzed 2 weeks after vector administration and already showed an extensive loss of DA neurons in the SNpc of animals expressing the human WT αSynuclein (43 ± 3%, compared with the non-injected control side). Only WT αSynuclein caused significant neuronal death at this early time point. Two weeks
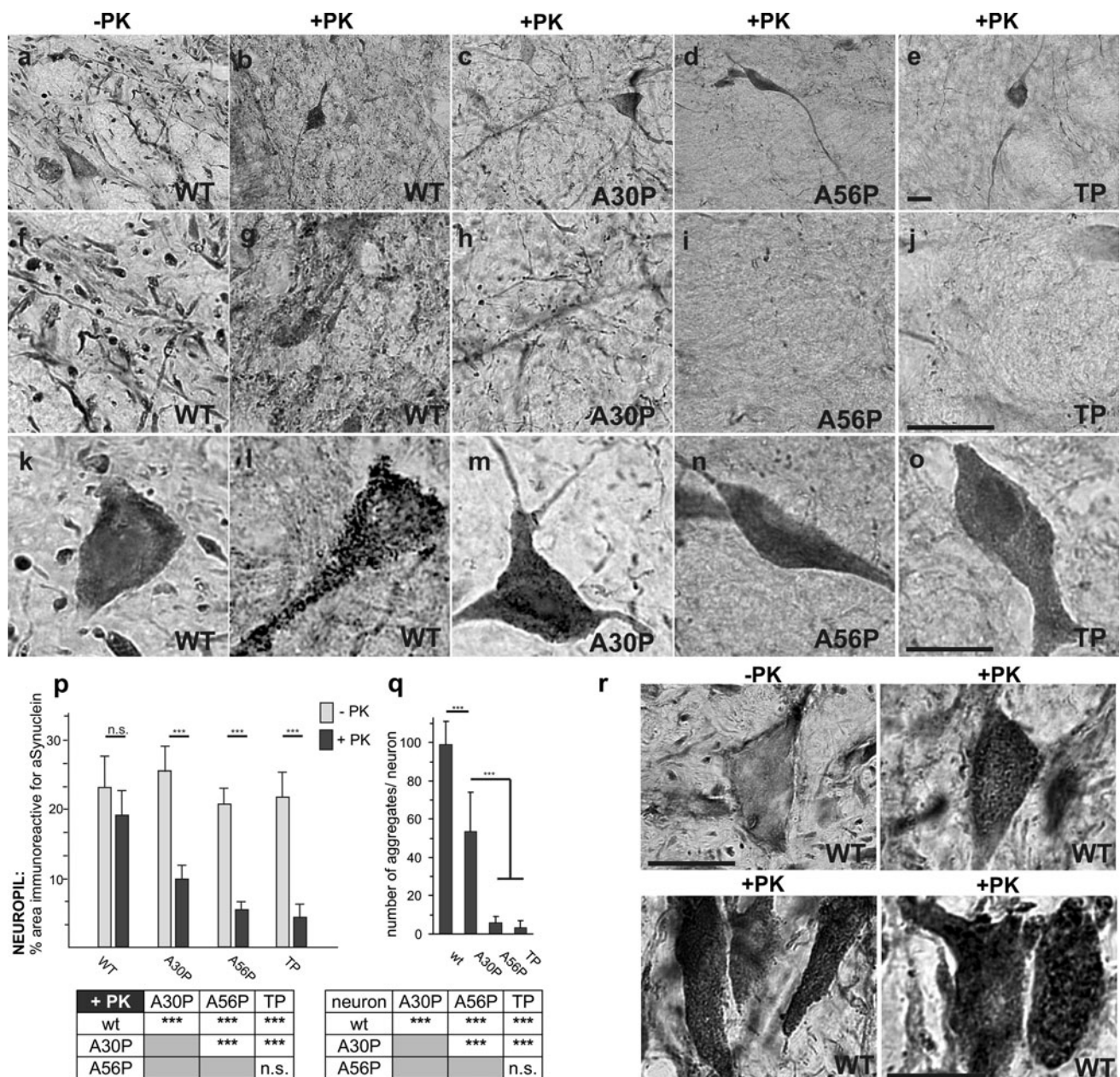
Fig. 2 αSynuclein immunoreactivity after PK digestion of SNpc tissue sections at 4 weeks after transduction: formation of PK-resistant αSynuclein aggregates in vivo. Staining against human αSynuclein in the SNpc after PK digestion (+PK) or without digestion (−PK). Overview in *upper panel* (**a**–**e**) and higher magnification of the neuropil in *middle panel* (**f**–**j**). Compared to WT αSynuclein (**g**), PK-resistant aggregates were less abundant in the nigral sections expressing the A30P (**h**) αSynuclein variant, and nearly absent for A56P (**i**) and TP (**j**). Lower panel (**k**–**o**) shows high-power images from cell somata of neurons, illustrating a dramatically increased number of small, dense inclusions for WT αSynuclein (**l**). Those cytoplasmic aggregates were less abundant in the nigral neurons expressing the A30P (**m**) αSynuclein variant, and nearly absent for A56P (**n**) and TP (**o**). *Scale bars* 15 μm. **p** Quantification of PK-resistant αSynuclein immunoreactive material in the neuropil of the SNpc 4 weeks after transduction. The difference between undigested (−PK) and digested (+PK) sections was highly significant for all αSynuclein variants except for WT (Welch Two Sample t test). Significant differences between PK-digested groups outlined below the graph (Tukey's, $p < 0.001$). **q** Number of PK-resistant, αSynuclein-immunoreactive aggregates per neuron. Significant differences between PK-digested groups outlined below the graph (Tukey's, $p < 0.001$). $n = 7$ for WT, $n = 8$ for A56P, $n = 14$ for A30P, $n = 5$ for TP. Data are presented as mean ± SD (**r**) Representative images showing neurons expressing the human WT αSynuclein 2 weeks post injection. PK-resistant aggregates had already developed. They were smaller in size and more numerous compared with aggregates 2 weeks later
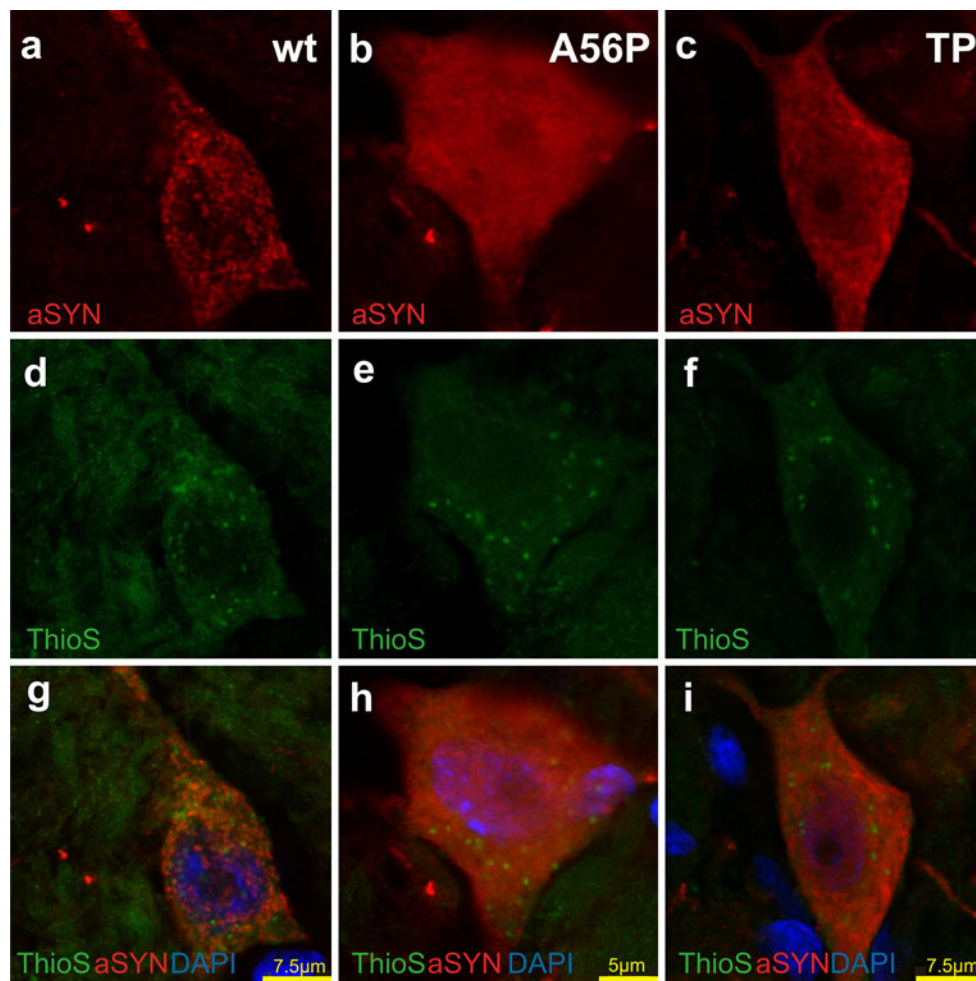
Fig. 3 PK-resistant aggregates of αSynuclein and ThioS-positive structures represent different entities in adult rat DA neurons. To further characterize PK-resistant aggregates, digested sections were immunofluorescently stained with a αSynuclein antibody, followed by a ThioS stain. We detected abundant ThioS-positive structures in DA neurons independent from αSynuclein expression, i.e., also in DA neurons of the contralateral nigra. However, these structures were in no case immunoreactive for aggregated αSynuclein, although we exploited several different αSynuclein antibodies (Syn211, aa121–135 of human αSynuclein; LB509, aa115–122, generated against Lewy bodies as immunogen; clone 42, aa 91–99 of rat and human αSynuclein; and 5C2, directed against the NAC domain). The figure shows ThioS/αSynuclein (Syn211 antibody, confocal detection) double staining after PK digestion (10 min, 55°C, 10 μg/ml) in SNpc 4 weeks after virus injection. DA neurons in the SN showed several small ThioS-positive inclusions (**d–f**) and many αSynuclein-positive aggregates (**a**), however, both structures did not colocalize (**g**). As shown before, neurons infected with WT αSynuclein (**a**) showed considerably more αSynuclein aggregates than neurons expressing A56P (**b**) or TP αSynuclein (**c**)

later, also the proline mutants of αSynuclein induced significant neurotoxicity. Four weeks after virus injection, we found that about 50% of DA neurons had degenerated in tissue expressing either WT (48 ± 17%), A56P (48 ± 8%) or TP (50 ± 7%) αSynuclein, while 27 ± 9% of DA neurons had died after expression of A30P αSynuclein (Fig. 4m). Thus, the prefibrillar αSynuclein mutants A56P and TP induced a similar extent of neurodegeneration as compared to WT αSynuclein at this time point. However, in contrast to results obtained in invertebrate and cellular models [22], prefibrillar αSynuclein did not aggravate DA neuron degeneration compared to WT αSynuclein.

Eight weeks post transduction, WT, A56P, and TP still produced a comparable extent of neurodegeneration (56 ± 19, 54 ± 12, 47 ± 8 and 31 ± 13% of DA neurons had degenerated through expression of WT, A56P, TP and A30P αSynuclein, respectively).

A fourth group of animals was analyzed 14 weeks after vector injections (Fig. 4a–m). In these brains, 69 ± 11% of DA neurons had degenerated in the WT group, and 39 ± 13% in the A30P group, demonstrating a progressive neuropathology. However, <50% DA neuron loss was detected in the A56P (42 ± 10) and TP (46 ± 8) groups (Fig. 4m), indicating that expression of these αSynuclein
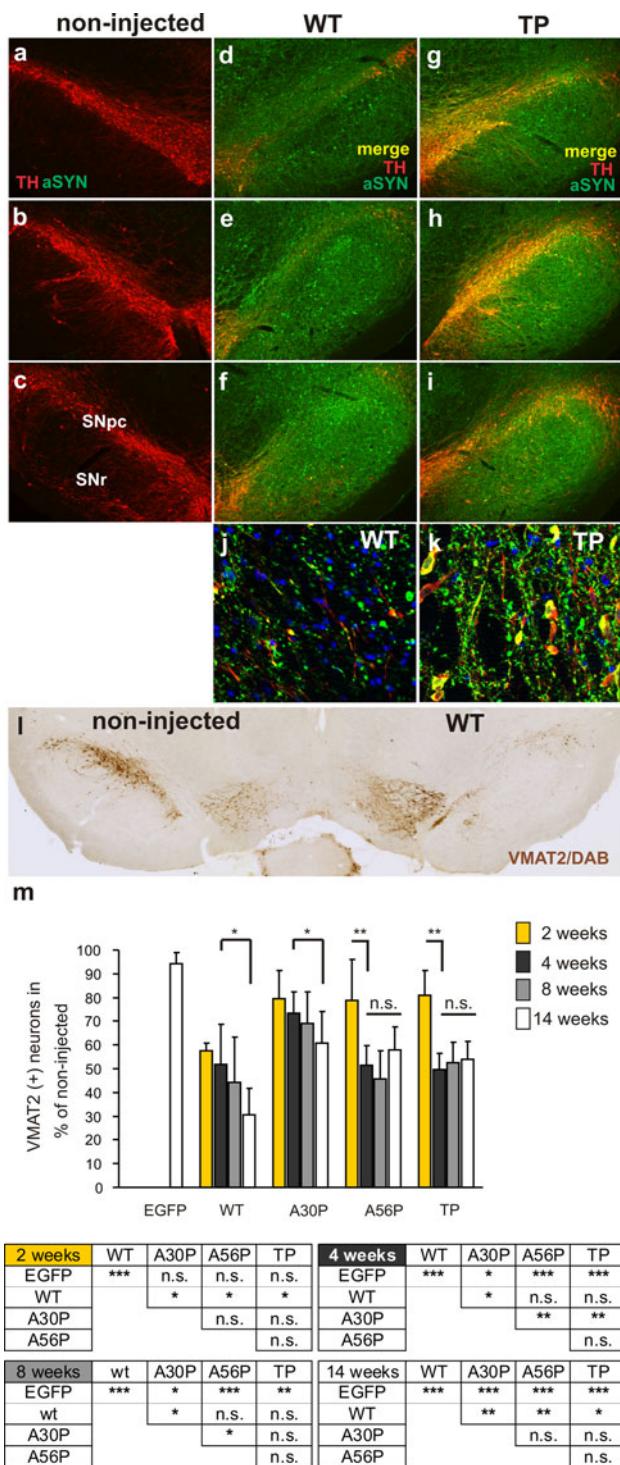
Fig. 4 Only fibrillar αSynuclein variants induce progressive DA neuron degeneration in vivo. **a–i** Representative images illustrating nigral DA neurodegeneration and significant overexpression of αSynuclein in the injected hemispheres by double staining for TH (*red*) and αSynuclein (*green*). Each column contains rostral-to-caudal coronal sections taken from the same animal and gives an overview of the extent of nigral DA neuron loss induced by expression of WT (**d–f**) or TP (**g–i**) αSynuclein at 14 weeks after AAV injection. Non-transduced control sections are shown in **a–c**. Higher magnification images (**j, k**) are optical sections of 1 μm and were generated with an ApoTome. DA cell bodies which demonstrated immunoreactivity for both, the DA marker TH and human αSynuclein, were found more frequently for TP than for WT. (**l**) Representative image of a coronal section showing nigral degeneration in a AAV-WT αSynuclein-injected animal. The nigral DA neurons were specifically labeled with an antibody against VMAT2 and with standard DAB immunohisto-chemistry. The expression of WT αSynuclein led to loss of VMAT2-positive neurons in the SNpc, compared with the contralateral intact side. **m** Changes in total number of VMAT2-positive cells in SNpc over time, as determined by stereology in the AAV-αSynuclein-WT, A30P, A56P, TP and AAV-EGFP-injected rats ($n = 5$–6 animals per time point and group). Data are shown as mean ± SD; significant differences between groups outlined below the graph (Tukey's test)

To determine whether the reduced number of DA cells in the SN was attributable to an actual loss of cells rather than to a downregulation of the cellular markers used, i.e., the TH enzyme and the VMAT2 protein, we used an antibody to the neuron-specific protein NeuN to label nigral neurons. The NeuN marker revealed a marked loss of SNpc cells on the AAV-αSynuclein-injected side, confirming that the neurons had indeed degenerated. Quantification of NeuN-positive cells in the SNpc of WT αSynuclein-injected animals 4 weeks post transduction revealed a 56% reduction compared to the non-injected side. Percentages of TH-positive cells among NeuN-positive cells were approximately 60% on the unlesioned side and increased on average to 68% on the injected sides, suggesting also a loss of non-DA neurons.

It should be noted that 14 weeks after application of AAV2-WT αSynuclein, we detected only few DA cell bodies which demonstrated immunoreactivity for both, the DA marker TH and human αSynuclein, while robust αSynuclein immunoreactivity persisted in the dystrophic remaining neuritis (Fig. 4j). In contrast, in TP and A56P expressing brains, many neuronal cell bodies were immunoreactive for TH and αSynuclein, suggesting that DA neurons overexpressing the prefibrillar αSynuclein variants can survive for long periods of time (Fig. 4k).

Fibrillar and prefibrillar αSynuclein variants are secreted from rat primary cortical neurons

αSynuclein is secreted from neurons via exocytosis [26] and αSynuclein-mediated neuropathology could be transmitted from affected to unaffected neurons [10]. To investigate whether progressive degeneration of WT and
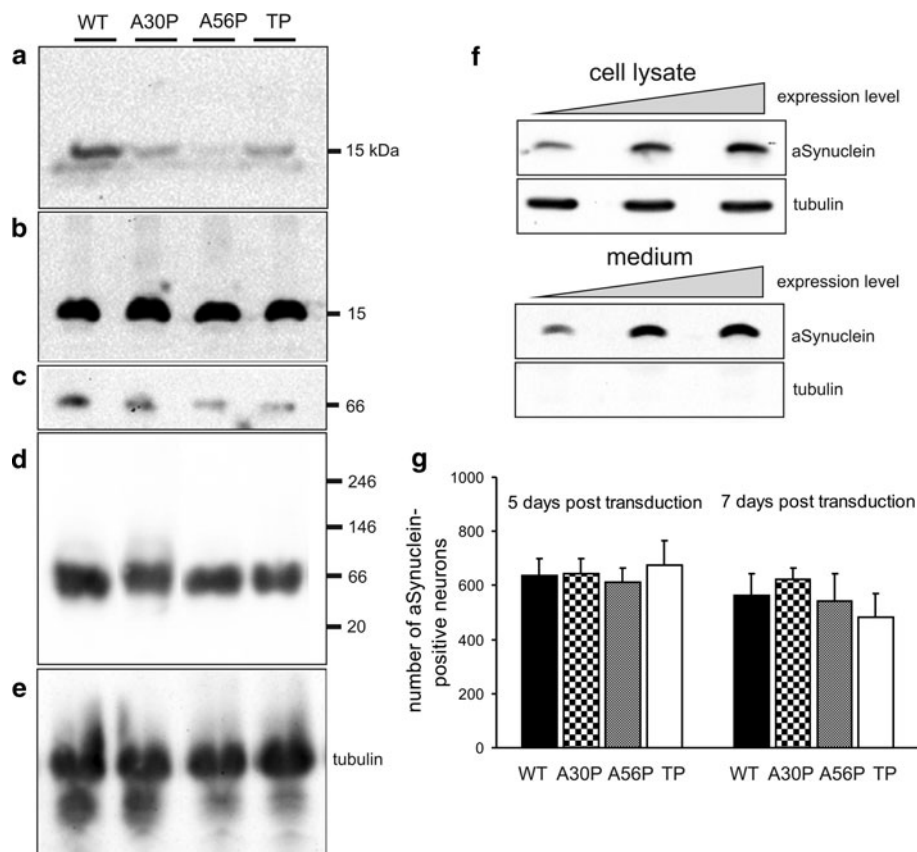
variants did not cause further progression of DA neuron degeneration. Instead, cell loss through expression of A56P and TP αSynuclein had already reached its maximum and final state at 4 weeks. Toxicity in these models could be entirely attributed to αSynuclein since EGFP controls showed only marginal evidence of degeneration 14 weeks post transduction (5.6 ± 4% cell loss).

Fig. 5 Secretion of overexpressed αSynuclein from primary cortical neurons. Cells were infected with the respective AAV vectors on day 3 in vitro. The conditioned medium and the cell lysates were collected at day 9 post transduction after 48 h of incubation in fresh medium. The conditioned medium (**a**) and the whole-cell extracts (**b**) of transduced cortical neurons were subjected to denaturing gel electrophoresis. Non-denaturing gel electrophoresis of αSynuclein from conditioned medium (**c**) and of αSynuclein isolated from cell pellet (**d**) with protein loading control (**e**). Molecular weight markers in kDa indicated on the *right*. Release of αSynuclein WT was enhanced compared with the other αSynuclein variants. **f** Secretion of αSynuclein correlates with its expression levels. Primary cortical neurons were transduced with three different titers of AAV-WT αSynuclein and the levels of intracellular (cell lysate) and released (medium) proteins were analyzed. Secreted proteins were collected for 48 h. In contrast to αSynuclein, tubulin was not released from the cells. **g** Neurotoxicity of WT and mutants of αSynuclein in rat primary cortical neurons transduced with AAV. Numbers of αSynuclein-positive neurons counted after transduction with respective αSynuclein variants. Expression of WT αSynuclein did not result in a lower number of surviving neurons compared with A30P, A56P and TP αSynuclein after 5 and 7 days, indicating that enhanced release of human WT αSynuclein into the medium was not the result of membrane leakage caused by cell death. Data are shown as mean ± SD

A30P transduced nigral DA neurons is related to enhanced secretion of αSynuclein, we overexpressed the αSynuclein variants in primary cultured neurons and quantified the amount of released αSynuclein in the culture medium. To collect the secreted proteins, the neurons were cultured in fresh medium for 48 h. The supernatant was analysed under denaturing and native conditions (Fig. 5a–e). Secreted αSynuclein was found to migrate as a single 14 kDa band under denaturing conditions, and at ∼60 kDa in gels when loaded without DTT/β-ME. αSynuclein WT, and all mutant variants were secreted from neurons. The highest amount was detected in the conditioned medium of WT-transduced cultures ($n = 5$ experiments), suggesting that enhanced secretion of human WT αSynuclein could contribute to the progressive degeneration induced by this variant.

The amount of released αSynuclein in the conditioned medium correlated with the intracellular expression levels of this protein (Fig. 5f). In the same set of cultures, endogenously expressed cytosolic protein tubulin was not detected in the culture medium, indicating that αSynuclein release was not the result of membrane leakage caused by cell death. To further corroborate that release of αSynuclein is not caused by dying neurons, we counted αSynuclein-positive neurons in primary cultures at 5, 7 and 9 days post transduction. No substantial decrease in cell number over time was detected. Since we found no sign of increased cell death in neurons overexpressing WT αSynuclein, we can exclude the possibility that the enhanced release of WT αSynuclein into the culture medium is attributable to membrane leakage (Fig. 5g).
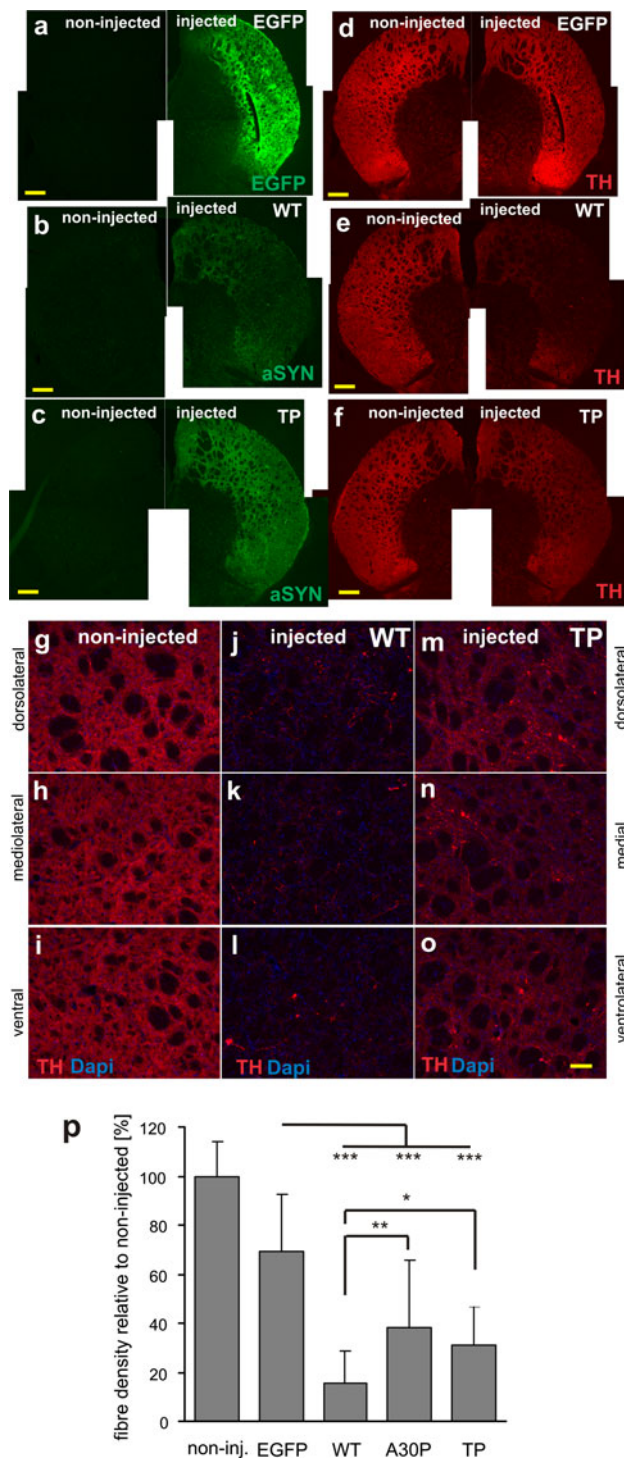
Fig. 6 Loss of TH-positive innervation in the striatum after expression of a fibrillar αSynuclein variant (WT) or the prefibrillar variant TP. Representative images illustrating the axonal fiber innervation in the striatum 14 weeks after AAV-mediated gene transfer into the SN. Overview of coronal sections showing transgene expression of EGFP (**a**), WT αSynuclein (**b**), and TP αSynuclein (**c**). Nigrostriatal fiber terminals in the striatum were filled with the transgenic protein. Immunohistochemical staining for TH (**d**–**f**) revealed that in contrast to the AAV-EGFP-injected animals (**d**), the expression of αSynuclein led to the appearance of degenerative changes and a loss of striatal fibers, which was more pronounced for WT (**e**). *Scale bar* 500 μm. **g**–**o** Higher magnification images covering the dorsal, medial and ventral area of a representative striatal section of an intact non-transduced control side (**g**–**i**), WT-transduced (**j**–**l**), and TP-transduced (**m**–**o**) brain. TH-immunostained sections showing the extent of loss of striatal innervation. Remaining fibers in the WT αSynuclein-treated animals were sparse. *Scale bar* 100 μm. **p** Quantification of fiber density revealed a clear reduction in TH-positive striatal innervation in the αSynuclein transduced animals at 14 weeks after injection (significant difference from the EGFP-transduced control group at $p < 0.001$). The difference between the WT and TP variant was also significant ($p = 0.048$), whereas the difference between A30P and TP was not

neurodegeneration, i.e., αSynuclein WT overexpression induced significantly more fiber loss as compared to TP and A30P overexpression (Fig. 6). αSynuclein immunoreactive striatal fibers displayed large numbers of dystrophic swollen profiles, which colocalized with the DA marker TH and morphologically differed considerably between WT, TP and A30P αSynuclein-expressing specimen (Fig. 7). Following WT overexpression, extensive beading of neuronal processes could be detected (Fig. 7a, d). In contrast, TP overexpression resulted in the appearance of large axonal retraction bulb-like structures, while the axon proximal to the retraction bulb showed fewer varicosities (Fig. 7b, e). A30P overexpression, which in nigral DA neurons resulted in fewer PK-resistant aggregates than WT but more such aggregates than TP, displayed an intermediate axonopathy. It induced fewer small, bead-like varicosities but more large retraction bulb-like profiles than WT αSynuclein (Fig. 7c, f). Thus, it appeared that aggregating αSynuclein WT resulted in extensive beading of neuronal processes, while less- and non-aggregating αSynuclein variants demonstrated a preference for generating large axonal retraction bulb-like structures. These results suggest that fibrillar and prefibrillar variants of αSynuclein induce different modes of axonopathy in nigral DA neurons.

Discussion

αSynuclein constitutes the major component of Lewy bodies and amyloid plaques [34], and its causal contribution to the etiology of Parkinson's disease is evident [16]. αSynuclein can adopt several oligomeric and fibrillar
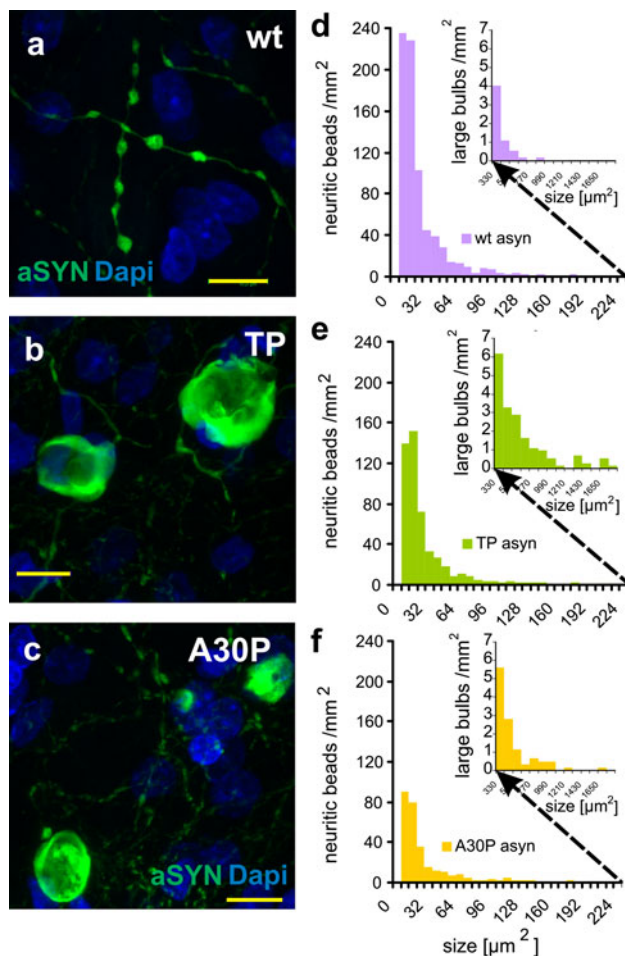
Differential striatal axonal pathology induced by αSynuclein fibrillar and prefibrillar variants

Nigral αSynuclein overexpression resulted in αSynuclein immunoreactivity in striatal projections of nigral DA neurons. The measured density of DA projections in the striatum correlated with the extent of nigral

Fig. 7 Distinctive axonal dystrophies detected in striatum after αSynuclein-WT, A30P or TP expression in nigral DA neurons. Representative examples of dystrophic axons in the striatum after expression of WT (**a**), TP (**b**) and A30P (**c**) αSynuclein. Immunohistochemistry with anti-αSynuclein antibody 5C2 against the NAC domain (*green*). Pictures show overlay with nuclear DAPI stain (*blue*). *Scale bar* 10 μm. Quantification of the sizes of TH-positive axonal swellings detected after αSynuclein-WT (**d**), TP (**e**) or A30P (**f**) expression. Note that the *x* axes are truncated and continue in the inserted *histogram* with a changed scale for the *y* axis to depict the quantification of large retraction bulbs as detected predominately after αSynuclein-TP expression. Quantitative data were extracted with the NIH MacBiophotonics ImageJ software with the analyze-particles function. Measurements were performed on one rostral and one caudal section for each brain. Numbers of counted structures: αSynuclein-WT, 4,178 objects from $n = 5$ animals; αSynuclein-TP, 3,837 objects from $n = 5$ animals; αSynuclein-A30P, 1,856 objects from $n = 4$ animals

conformation states, but it is still uncertain which of the different conformational states of αSynuclein mediate neurotoxicity. The present study was motivated by recent results showing that rationally designed mutants of αSynuclein showed dramatically reduced propensity to form insoluble aggregates in solution and in *C. elegans*, and that these variants of αSynuclein demonstrated enhanced

neurotoxicity in mammalian cell lines, Drosophila, *C. elegans* and cultured rat DA neurons [22]. These results were interpreted as a confirmation of the "toxic oligomer" hypothesis in the sense that the primary toxic species of αSynuclein are prefibrillar, putatively soluble oligomeric conformations.

Extensive biophysical analysis demonstrated that the point mutations neither alter the structural properties of the protein as monomer in solution, nor prohibit the formation of an α-helical conformation on the surface of SDS micelles, but strongly differed in their ability to form amyloid fibrils. All variants efficiently bind to phospholipid vesicles. The vesicle affinity of A56P or TP αSynuclein was very similar to that observed for A30P [22].

We report on a rat model using AAV2 delivery of αSynuclein that differs in the rate of progression and severity in DA pathology based on the variant of AAV2-αSynuclein injected. Human-WT αSynuclein caused a rapid onset of nigral pathology (within 2 weeks), including the abundant presence of PK-resistant aggregates of αSynuclein, and a continuous progressive loss of DA neurons between 2 and 14 weeks. Expression of A30P αSynuclein also caused a gradually progressive loss of DA neurons, but with a later onset compared to WT. The prefibrillar αSynuclein variants produced initially only marginal signs of toxicity (at 2 weeks) followed by a dramatic DA cell death at 4 weeks, however, without further progression. Thus, interestingly, the non-aggregating αSynuclein variants showed clearly different kinetics of toxicity compared to those αSynuclein variants that are able to form fibrils (WT and A30P). Taken together, our results highlight a possible link between fibrillization of αSynuclein and progressive neurodegeneration. We are neither suggesting that the propensity of αSynuclein to aggregate is the only property nor that it is the main property of the protein causing DA neurodegeneration, but our results clearly indicate that aggregation plays a major role in the progression of DA cell loss and that aggregation-impaired mutants have lost the ability to trigger a sustained neurodegeneration.

We demonstrate that the prefibrillar αSynuclein variants A56P and TP form fewer PK-resistant aggregates as compared to WT αSynuclein and the familial A30P mutation, not only in cultured primary cortical rat neurons but also in neurites and cell bodies of adult nigral DA neurons in vivo. Thus, these proteins behaved in vivo as predicted by biophysical assessments in defined solutions [22]. However, in contrast to cell culture and invertebrate models, the prefibrillar mutants did not amplify αSynuclein-related degeneration of rat DA neurons in vivo as compared to the WT protein. Whereas at 4 and 8 weeks after viral-vector application cell death was still comparable between fibrillar WT αSynuclein and prefibrillar

variants, WT was the most toxic variant after 14 weeks of expression. Among the mutants, A56P and TP caused a stronger cell loss at 4 and 8 weeks, but they were neither in the beginning (2 weeks) nor at a later stage (14 weeks) more toxic than A30P. Thus, already after 4 weeks, the neurotoxic effect of the prefibrillar mutants appeared to have subsided, because after an initial insult the remaining neurons survived despite the fact that the level of αSynuclein expression remained high. These results show that nigral DA neurons were vulnerable to high levels of either WT or mutant αSynuclein, however, only the fibril-forming WT and A30P variants of αSynuclein caused a progressive form of DA neuron degeneration.

The discrepancy between our current results and previous work conducted in invertebrate models and cultured primary neurons [22] with respect to αSynuclein toxicity highlights the necessity to confirm studies that investigate the neurotoxic consequences of αSynuclein aggregation also in adult mammalian DA neurons in vivo. Given that αSynuclein is a very abundant protein in mammalian brain [19] it is likely that mammalian neurons have developed mechanisms to modulate αSynuclein aggregation, which do not exist in invertebrate neurons. Furthermore, our current results demonstrate that even in rat DA neurons, in vivo expression of oligomeric versus fibril-forming αSynuclein variants can lead to divergent results. In a recent study [44], it was shown that artificial mutants disrupting salt bridges between β-strands of αSynuclein (E35K or E57K) generated more oligomers and less fibrils than WT or A30P αSynuclein in aggregation assays under certain conditions (but more fibrils under different conditions), and that these mutants were significantly more toxic than WT or A30P αSynuclein for rat DA neurons in vivo. Thus, differences in experimental design with respect to the nature of the αSynuclein mutations (disrupting salt bridges between β-strands through lysine substitutions [44] versus directly disrupting β-sheets through proline substitutions [22]), viral-vector system and promoter, duration of transgene expression, and readout of aggregate formation in vivo make it difficult to evaluate the toxic oligomer hypothesis, and warrant further studies under more matching conditions.

Progressive neurodegeneration and its correlation to the formation of PK-resistant aggregates were assessed in our current study for the first time. The composition of PK-resistant αSynuclein aggregates is incompletely defined but ample evidence suggests that they consist at least partially of fibrillar αSynuclein. αSynuclein fibrils generated in vitro [8, 14, 30, 33], and fibrillar αSynuclein in the detergent-insoluble fraction of human synucleinopathy brains are resistant to PK digestion [30, 33]. In contrast, small-sized oligomers are not PK-resistant as recently shown in brain lysates of A53T transgenic mice [40]. Colocalization of αSynuclein aggregates with the classical amyloid stain

ThioS has been reported [2] but it was absent in many other studies [21, 24, 25, 31]. Such colocalization may crucially depend on the accessibility of exposed grooves, which are rich in aromatic residues, on the surface of amyloid fibrils [5]. Despite the missing colocalization with ThioS, the resistance of aggregates of WT or A30P αSynuclein to PK is in agreement with a very stable structure as found in amyloid fibrils.

We report here that fibrillar and prefibrillar αSynuclein variants caused divergent axonal pathologies, further exemplifying that they induce neurotoxicity by different means. Degenerating axons of WT αSynuclein expressing DA neurons displayed a multitude of small varicosities of about 30–50 μm² area, but very few large retraction bulb-like profiles larger than 300 μm² in size. Conversely, axons of TP αSynuclein-expressing DA neurons demonstrated fewer small varicosities but more large retraction bulb-like profiles. Thus, axonal transport and/or structural integrity appear to be differentially affected by the presence of αSynuclein variants which are impaired in fibrillation (A56P/TP) as compared to those variants which have high propensity to form fibrils (WT/A30P).

In our rodent model, the familial A30P mutant was found to be less toxic than human WT αSynuclein at all investigated time points. This is in agreement with another rat model using rAAV2/6-mediated expression of αSynuclein in which WT αSynuclein displayed stronger toxicity than the A30P mutant when assayed 8 weeks post-virus injection [2]. Even though WT and A30P are both fibrillar αSynuclein variants, we provided evidence that A30P is less likely to aggregate in vivo, which is in agreement with many other studies showing that A30P does form fibrils, but fibrillizes more slowly than WT [9, 28]. This could explain, at least in part, the differences in toxicity between these αSynuclein variants, but is most likely not the only reason. The A30P mutation reduces the affinity of αSynuclein for biological membranes and this may have an impact on pathophysiological effects [1]. Indeed, it has been shown that the A30P mutant fails to impair the growth of yeast cells [35].

Our models demonstrate that αSynuclein overexpression for 4 weeks is sufficient to trigger significant nigral DA cell loss independent of the αSynuclein species. Two weeks after transduction, both the fibrillar as well as prefibrillar proline mutants showed only marginal evidence of degeneration. After 4 and 8 weeks of overexpression, A56P and TP displayed higher toxicity than the A30P mutation. This could be taken as an argument for the toxic oligomer. Nevertheless, at 14 weeks post transduction, the A30P mutant had already reached the same toxic effect as A56P and TP. Those αSynuclein species that have the potential to trigger a gradual progression of neurodegeneration are likely to be the most toxic at long term, even if they do not cause the highest cell loss at intermediate time points. It was

reported that A30P induced a time-dependent degeneration process and that at 5 months expression, A30P had caused the same loss of TH-positive nigral neurons as WT αSynuclein [29]. Another study also detected no significant difference in loss of TH-positive neurons between WT and A30P [44]. Likewise, a study in mice did not find any obvious difference in pathogenicity between the WT and A30P mutant form of αSynuclein [25] implying that A30P can induce the same extend of neuronal loss as WT.

We hypothesize that the ability of αSynuclein to form fibrils is required for progressive neurodegeneration. The A53T variant of αSynuclein has an increased aggregation propensity in vitro and forms fibrils more quickly than human WT αSynuclein [28]. The finding that AAV-mediated overexpression of mutant A53T αSynuclein results in progressive, time-dependent DA neuron loss in rats is consistent with our idea. In animals given either WT or A53T αSynuclein, the pathological changes were similar, both quantitatively and qualitatively [23] and the authors noted a similar appearance of αSynuclein-positive cytoplasmic inclusions and granular deposits as described in the present study. In a different report, overexpression of A53T αSynuclein in the rat nigra resulted in protracted, but nevertheless progressive neurodegeneration [7]. The delayed degeneration may be related to the fact that human A53T corresponds to WT αSynuclein in rodents. The demonstrated gradual loss of DA cell bodies in the SN caused by the fibrillar mutant A53T is in agreement with our conclusion, that αSynuclein fibril formation is not an epiphenomenon but mechanistically involved in progressive neurodegeneration.

In conclusion, generation of both soluble oligomers and PK-resistant aggregates of αSynuclein leads to death of mammalian DA neurons in vivo, but formation of PK-resistant aggregates is required for the induction of progressive degeneration of DA neurons as found in PD patients. The formation of PK-resistant fibrillar aggregates may thus represent the critical pathomechanism that needs to be targeted to achieve a slowing down of the progression of PD and related synucleinopathies.

References

1. Auluck PK, Caraveo G, Lindquist S (2010) Alpha-Synuclein: membrane interactions and toxicity in Parkinson's disease. Annu Rev Cell Dev Biol 26:211–233
2. Azeredo da Silveira S, Schneider BL, Cifuentes-Diaz C et al (2009) Phosphorylation does not prompt, nor prevent, the formation of alpha-synuclein toxic species in a rat model of Parkinson's disease. Hum Mol Genet 18:872–887
3. Bartels T, Choi JG, Selkoe DJ (2011) Alpha-Synuclein occurs physiologically as a helically folded tetramer that resists aggregation. Nature 477:107–110
4. Beach TG, White CL, Hamilton RL et al (2008) Evaluation of alpha-synuclein immunohistochemical methods used by invited experts. Acta Neuropathol 116:277–288
5. Biancalana M, Koide S (2010) Molecular mechanism of thioflavin-T binding to amyloid fibrils. Biochim Biophys Acta 1804:1405–1412
6. Caughey B, Lansbury PT (2003) Protofibrils, pores, fibrils, and neurodegeneration: separating the responsible protein aggregates from the innocent bystanders. Annu Rev Neurosci 26:267–298
7. Chung CY, Koprich JB, Siddiqi H, Isacson O (2009) Dynamic changes in presynaptic and axonal transport proteins combined with striatal neuroinflammation precede dopaminergic neuronal loss in a rat model of AAV alpha-synucleinopathy. J Neurosci 29:3365–3373
8. Conway KA, Harper JD, Lansbury PT Jr (2000) Fibrils formed in vitro from alpha-synuclein and two mutant forms linked to Parkinson's disease are typical amyloid. Biochemistry 39:2552–2563
9. Conway KA, Lee SJ, Rochet JC, Ding TT, Williamson RE, Lansbury PT Jr (2000) Acceleration of oligomerization, not fibrillization, is a shared property of both alpha-synuclein mutations linked to early-onset Parkinson's disease: implications for pathogenesis and therapy. Proc Natl Acad Sci USA 97:571–576
10. Desplats P, Lee HJ, Bae EJ et al (2009) Inclusion formation and neuronal cell death through neuron-to-neuron transmission of alpha-synuclein. Proc Natl Acad Sci USA 106:13010–13015
11. Devine MJ, Gwinn K, Singleton A, Hardy J (2011) Parkinson's disease and alpha-synuclein expression. Mov Disord 26(12):2160–2168
12. Fernagut PO, Hutson CB, Fleming SM et al (2007) Behavioral and histopathological consequences of paraquat intoxication in mice: effects of alpha-synuclein over-expression. Synapse 61:991–1001
13. Fink AL (2006) The aggregation and fibrillation of alpha-synuclein. Acc Chem Res 39:628–634
14. Giasson BI, Murray IV, Trojanowski JQ, Lee VM (2001) A hydrophobic stretch of 12 amino acid residues in the middle of alpha-synuclein is essential for filament assembly. J Biol Chem 276:2380–2386
15. Gibb WR, Lees AJ (1988) The relevance of the Lewy body to the pathogenesis of idiopathic Parkinson's disease. J Neurol Neurosurg Psychiatry 51:745–752
16. Hardy J (2010) Genetic analysis of pathways to Parkinson disease. Neuron 68:201–206
17. Hardy J, Lewis P, Revesz T, Lees A, Paisan-Ruiz C (2009) The genetics of Parkinson's syndromes: a critical review. Curr Opin Genet Dev 19:254–265
18. Hindle JV (2010) Ageing, neurodegeneration and Parkinson's disease. Age Ageing 39:156–161
19. Iwai A, Masliah E, Yoshimoto M et al (1995) The precursor protein of non-A beta component of Alzheimer's disease amyloid is a presynaptic protein of the central nervous system. Neuron 14:467–475

20. Jellinger KA (2003) Neuropathological spectrum of synuclein-opathies. Mov Disord 18(Suppl 6):2–12
21. Kallhoff V, Peethumnongsin E, Zheng H (2007) Lack of alpha-synuclein increases amyloid plaque accumulation in a transgenic mouse model of Alzheimer's disease. Mol Neurodegener 2:6
22. Karpinar DP, Balija MB, Kügler S et al (2009) Pre-fibrillar alpha-synuclein variants with impaired beta-structure increase neurotoxicity in Parkinson's disease models. EMBO J 28:3256–3268
23. Kirik D, Rosenblad C, Burger C et al (2002) Parkinson-like neurodegeneration induced by targeted overexpression of alpha-synuclein in the nigrostriatal system. J Neurosci 22:2780–2791
24. Klein RL, King MA, Hamby ME, Meyer EM (2002) Dopaminergic cell loss induced by human A30P alpha-synuclein gene transfer to the rat substantia nigra. Hum Gene Ther 13:605–612
25. Lauwers E, Debyser Z, Van Dorpe J, De Strooper B, Nuttin B, Baekelandt V (2003) Neuropathology and neurodegeneration in rodent brain induced by lentiviral vector-mediated overexpression of alpha-synuclein. Brain Pathol 13:364–372
26. Lee HJ, Patel S, Lee SJ (2005) Intravesicular localization and exocytosis of alpha-synuclein and its aggregates. J Neurosci 25:6016–6024
27. Leong SL, Cappai R, Barnham KJ, Pham CL (2009) Modulation of alpha-synuclein aggregation by dopamine: a review. Neurochem Res 34:1838–1846
28. Li J, Uversky VN, Fink AL (2001) Effect of familial Parkinson's disease point mutations A30P and A53T on the structural properties, aggregation, and fibrillation of human alpha-synuclein. Biochemistry 40:11604–11613
29. Lo Bianco C, Ridet JL, Schneider BL, Deglon N, Aebischer P (2002) Alpha-Synucleinopathy and selective dopaminergic neuron loss in a rat lentiviral-based model of Parkinson's disease. Proc Natl Acad Sci USA 99:10813–10818
30. Miake H, Mizusawa H, Iwatsubo T, Hasegawa M (2002) Biochemical characterization of the core structure of alpha-synuclein filaments. J Biol Chem 277:19213–19219
31. Morales R, Estrada LD, Diaz-Espinoza R et al (2010) Molecular cross talk between misfolded proteins in animal models of Alzheimer's and prion diseases. J Neurosci 30:4528–4535
32. Mori F, Tanji K, Yoshimoto M, Takahashi H, Wakabayashi K (2002) Demonstration of alpha-synuclein immunoreactivity in neuronal and glial cytoplasm in normal human brain tissue using proteinase K and formic acid pretreatment. Exp Neurol 176:98–104
33. Neumann M, Kahle PJ, Giasson BI et al (2002) Misfolded proteinase K-resistant hyperphosphorylated alpha-synuclein in aged transgenic mice with locomotor deterioration and in human alpha-synucleinopathies. J Clin Invest 110:1429–1439
34. Nussbaum RL, Ellis CE (2003) Alzheimer's disease and Parkinson's disease. N Engl J Med 348:1356–1364
35. Outeiro TF, Lindquist S (2003) Yeast cells provide insight into alpha-synuclein biology and pathobiology. Science 302:1772–1775
36. R DCT (2010) R: a language and environment for statistical computing. R Foundation for Statistical Computing, Vienna. http://www.R-project.org
37. Shevtsova Z, Malik I, Garrido M, Schöll U, Bähr M, Kügler S (2006) Potentiation of in vivo neuroprotection by BclX(L) and GDNF co-expression depends on post-lesion time in deafferentiated CNS neurons. Gene Ther 13:1569–1578
38. Shevtsova Z, Malik JM, Michel U, Bähr M, Kügler S (2005) Promoters and serotypes: targeting of adeno-associated virus vectors for gene transfer in the rat central nervous system in vitro and in vivo. Exp Physiol 90:53–59
39. Sun A, Nguyen XV, Bing G (2002) Comparative analysis of an improved thioflavin-s stain, Gallyas silver stain, and immunohistochemistry for neurofibrillary tangle demonstration on the same sections. J Histochem Cytochem 50:463–472
40. Tsika E, Moysidou M, Guo J et al (2010) Distinct region-specific alpha-synuclein oligomers in A53T transgenic mice: implications for neurodegeneration. J Neurosci 30:3409–3418
41. Uversky VN, Eliezer D (2009) Biophysics of Parkinson's disease: structure and aggregation of alpha-synuclein. Curr Protein Pept Sci 10:483–499
42. Walsh DM, Selkoe DJ (2004) Oligomers on the brain: the emerging role of soluble protein aggregates in neurodegeneration. Protein Pept Lett 11:213–228
43. West MJ, Slomianka L, Gundersen HJ (1991) Unbiased stereological estimation of the total number of neurons in thesubdivisions of the rat hippocampus using the optical fractionator. Anat Rec 231:482–497
44. Winner B, Jappelli R, Maji SK et al (2011) In vivo demonstration that alpha-synuclein oligomers are toxic. Proc Natl Acad Sci USA 108(10):4194–4199
45. Yu S, Zuo X, Li Y et al (2004) Inhibition of tyrosine hydroxylase expression in alpha-synuclein-transfected dopaminergic neuronal cells. Neurosci Lett 367:34–39
46. Zhang NY, Tang Z, Liu CW (2008) Alpha-Synuclein protofibrils inhibit 26 S proteasome-mediated protein degradation: understanding the cytotoxicity of protein protofibrils in neurodegenerative disease pathogenesis. J Biol Chem 283:20288–20298
47. Zhu M, Fink AL (2003) Lipid binding inhibits alpha-synuclein fibril formation. J Biol Chem 278:16873–16877